Central Mindanao University
Journal of Science
ISSN Print: 0116-7847 ISSN Online: 2704-3703

Remote Sensing Technology Application for Tree Plantation Characterization and Sustainable Operation

Olpenda, A. S.[a], Paquit, J. C.[b], Tulod, A. M.[b], Polinar, K. D.[b] and R. G. Aguinsatan[a]

[a]Forest Resources Management Department
[b]Forest Biological Sciences Department
College of Forestry and Environmental Science
Central Mindanao University, Musuan, Bukidnon, Philippines 8710

ABSTRACT

In order to increase the supply of timber especially from industrial tree plantations (ITPs) and at the same time reducing the pressure on the remaining natural forests, proper planning and management must be strengthened. A plantation manager can efficiently do this if equipped with the right information using the latest but cost-efficient technology. This study was conducted to show the usefulness of remote sensing datasets in approximating the spatial distribution of the relative amount of wood materials in a *Gmelina arborea* Roxb. plantation and in identifying site parameters significant to the growth and development of the plantation. Between October 2019 and March 2020, field inventory was conducted within the *G. arborea* plantation of CMU in Bukidnon. A total of 38 randomly generated circular plots of 15-m radius were established. All tree and stand parameters inside the plots were subjected to correlation with 13 vegetation indices and 7 bands derived from Sentinel-2 (S2) multispectral image. Findings revealed that all but one of the indices were statistically correlated with the mean height, stem volume and basal area (BA) with their respective highest R values of 0.59, 0.65 and 0.66 ($p<0.01$). The Leaf Chlorophyll Index (LCI), after subjecting to curve estimation modeling, was able to explain the variation of the field data at 43% and 41% for stem volume and BA, respectively with standard errors of estimate of 0.40 and 0.34. It is suggested that more samples should be added in the analysis and use a non-parametric regression technique which may improve the model.

Keywords: *Gmelina arborea*, tree plantation, Sentinel-2, vegetation index, Bukidnon

INTRODUCTION

Tree farming is an alternative livelihood for many farmers in Mindanao and has been a significant option to meet the increasing demand for wood in the region while reducing the pressure on the remaining natural forests. However, proper planning and management must be strengthened to increase the supply of wood especially from industrial tree plantations (ITPs). A plantation manager can effectively do this if equipped with the right information using the latest but cost-efficient technology. These information includes, among others, canopy height, estimated volume, stand density or basal area that may represent harvestable woody materials. These tree parameters can be obtained from the field using the traditional inventory technique. As reliable as it may be, such technique is expensive and laborious.

The ITP of Central Mindanao University (CMU) in Bukidnon, composed chiefly of fast-growing exotic trees, has an area of 575.16 hectares (CMU CLUP, 2016) wherein the largest area is occupied by *Gmelina arborea* (about 371.15 ha or 64.5% of the total tree plantation area). This prime ITP species has been gaining popularity not only because it is used for posts, house timber or as a material for veneer and plywood, but also as a substitute for banned forest wood, particularly for use in the furniture industry (DOST-PCAARRD, 2018). The tree plantation is one the University's income-generating projects that addresses lumber demands of CMU itself, its constituents, and even nearby towns for building and house construction. In spite of its critical role, a map of the plantation with reference to the latest inventory is lacking. A visual presentation of the ITP with blocking grids based on certain stand parameters would be ideal for a more organized and systematic logging operation.

The technology of remote sensing (RS) is a powerful tool in assessing vegetation properties at different scales and objectives. This paper utilized specifically passive RS which relies on natural energy (normally from the sun) that is reflected or emitted by the Earth's surface. This technique had been used by a number of authors using optical sensors onboard satellites for forest biomass estimation (Nguyen et al, 2020), refo- and deforestation analysis (Perez et al, 2020), predicting forest structures (Gebreslasie et al, 2020) and forest fire assessment (Olpenda, 2019). Dos Reis et al (2018) were able to generate correlation values of -0.91 for basal area and -0.52 for tree volume of Eucalyptus trees using band ratios of Landsat TM with 30m spatial resolution. Benguet et al (2012) on the other hand produced better results in estimating forest structures (R2 up to 0.97) by using a very high resolution satellite images. Meanwhile, Günlü and Kadıoğulları (2018) were able to directly compare the performance of low

Corresponding author:
Olpenda, A. S.
Email Address: alecsolpenda@cmu.edu.ph
Received: Jan. 19, 2022 ; Accepted: Oct. 23, 2023

and high resolution images to predict the basal area of pine forest using vegetation indices. From their research, vegetation indices derived from Landsat and Quickbird datasets produced R2 values of 0.36 and 0.54, respectively for stand volume prediction. Meanwhile, Brown et al (2022) combined lidar, an active type of remote sensing that uses laser technology, and Sentinel-2 in estimating forest metrics of mixed stands. The results of their study suggest that the addition of multispectral imagery is not significantly useful in improving the estimates of BA and volume. Based on these literatures and similar studies, the accuracy of the model depends on the types of sensors used, spatial resolutions of the dataset as well as the conditions of the forest (e.g. age, heterogeneity, stand density).

Although there are already a number of studies conducted in CMU's tree plantation and natural forest areas (e.g., Olpenda and Tulod, 2019; Rojo and Paquit, 2018; Tulod et al, 2017), the application of RS technology is very scarce. Maps generated from satellite images, coupled with field data, are advantageous for inaccessible sites and require less resources in the long run. The primary purpose of this study therefore is to explore the usefulness of RS data in approximating the spatial distribution of the relative amount of wood materials in a tree plantation. The results are expected to have sustainable management implications especially in the use of RS technology as a tool to track the development of tree plantations in the area for adaptive management.

METHODOLOGY

Study Area

The area of the study is the plantation of *G. arborea* (local name: yemane) of CMU, located mostly at the northwestern side of its titled land along Sayre Highway, Maramag, Bukidnon. CMU lies between 125°03'03" E longitude and 7°51'34'' N latitude and is situated 4.5 kilometers south of the city of Valencia. Based on the University's Comprehensive Land Use Plan (2016), the total area of the said plantation is 371.15 ha with an elevation ranging from 305 to 669 meters above sea level. Natural forest of secondary growth and agricultural land uses mostly surround the plantation forests. Other ITP species in the area include *Swietenia macrophylla*, *Acacia mangium* and *Tectona grandis*. On the other hand, majority of CMU's land area has a slope of less than 10% and for the G. arborea plantation alone, about 80% of its area has a slope of 8 to13%. In terms of climate, the area falls under Type III based on the Modified Corona classification of PAGASA. Type III climate is characterized as having a seasonal variability that is not very well pronounced, with dry season from November to April and wet during the remaining months of the year.

Sampling Plots

Sampling plots for this study were randomly

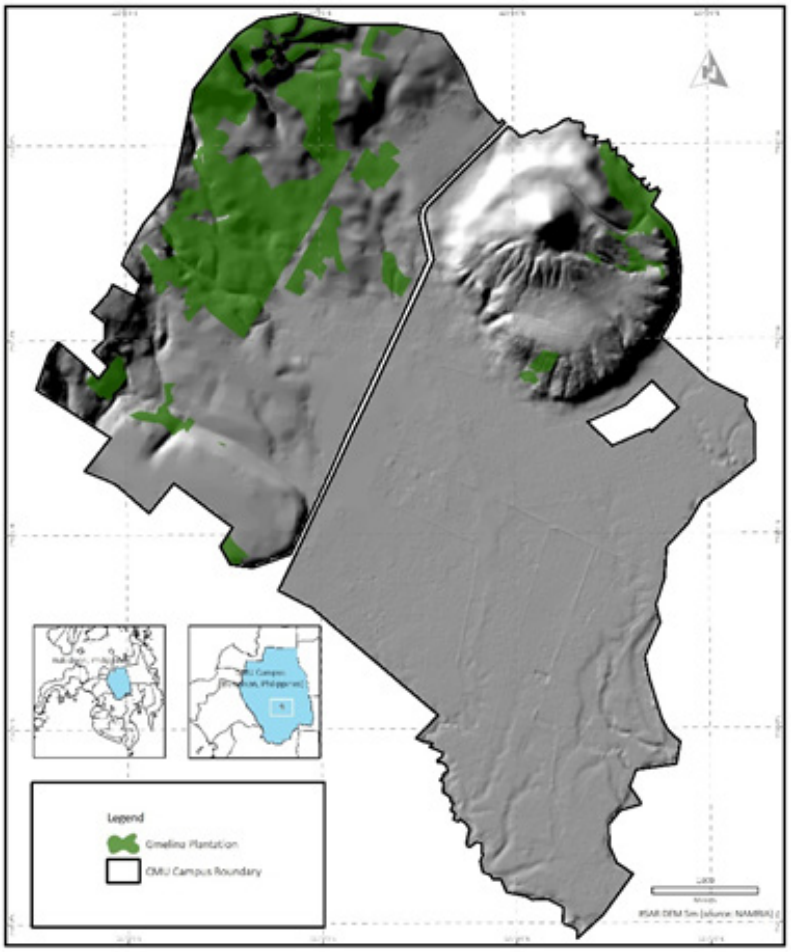

Figure 1. Location of the study area with hillshaded depiction of the terrain as basemap

generated using GIS. A total of 38 circular plots with 15 m radius and equivalent area of 0.07 ha. were established. The exact coordinates of these plots were taken from the field using survey-grade GPS equipment (up to 20cm accuracy) at the center of each individual plot. All field measurements were conducted between October 2019 and March 2020.

Field Inventory

The following tree and stand parameters were recorded during the fieldwork: diameter at breast (DBH) using tree calipers, merchantable height (MH, from stump to the first live branch) and the total height (TH, from stump to the apical tip of the tree) using a digital hypsometer or Haga altimeter. Only trees with a DBH of 10 cm or greater were included in the inventory. From the collected data, other plot-level parameters were calculated (equations 1 – 3). Basal area (BA) was later converted to the standard unit of density (m2/hectare). BA is important in this study because it's a good indicator of the presence of trees quantitatively. Stem volume on the other hand was calculated in two ways: (1) those with only pure main stem by using the MH as the multiplier (to be called SVMH) and (2) main stem plus the crown length by using the TH where branches and leaves are present (to be called SVTH). Crown length (CL) was also included in the analysis since it signifies the condition of the crown relative to the amount of branches and leaves. Additionally, the canopy cover for each plot, defined as the percentage area above ground covered by the leaves, branches and trunks of all trees, was taken from the averaged visual estimates of three persons conducting the fieldwork.

$$Basal\ area\ (BA) = 3.1416\left(\frac{DBH}{2}\right)^2 \quad \text{Eq. (1)}$$

$$Stem\ volume\ (SV) = 3.1416\ (DBH)(MH\ or\ TH) \quad \text{Eq. (2)}$$

$$Crown\ lenght\ (CL) = TH - MH \quad \text{Eq. (3)}$$

Remote Sensing (RS) Data

Sentinel-2 (S2) from the Multi Spectral Instrument (MSI) of the European Space Agency (ESA) was used for the analysis. The full S2 mission comprises twin polar-orbiting satellites in the same orbit (Sentinel-2A and Sentinel-2B), phased at 180° to each other. The mission monitors variability in land surface conditions, and its wide swath width and high revisit time (10 days at the equator with one satellite, and 5 days with 2 satellites under cloud-free conditions which results in 2-3 days at mid-latitudes) will support monitoring of changes to vegetation within the growing season (ESA, 2015). The sensor has 13 spectral bands ranging from 443 to 2,190 nm with spatial resolutions of 10 m (3 visible and 1 near-infrared (NIR) bands), 20 m (4 red edge and 2 shortwave infrared (SWIR) bands) and 60 m (3 atmospheric correction bands) (figure 2). Red edge bands are known to be sensitive to the health and condition of any vegetation in general (Curran et al., 1990; Gitelson et al., 1996; Richardson et al., 2002).

The original 100 km2 tile of S2 imagery utilized in this study was downloaded from the Copernicus Sentinel Scientific Data Hub website (https://scihub.copernicus.eu/) and has an acquisition date of 23 December 2019. It was then sub-sampled to cover only the cloud-free area of interest for the study site (figure 3). The dataset was in L2A level format, which is already an orthorectified Bottom-of-Atmosphere (BoA) corrected reflectance product.

Generation of Vegetation Indices

Various spectral vegetation indices (VIs) were computed from the bands of the S2 image using the raster calculator in Quantum GIS software (ver. 3.16.9). These indices, generated through mathematical equations and transformations (table 1), are computationally simple and easy to implement while capturing a wide range of vegetation biophysical variables (Xie et al., 2015). A total of 9 vegetation indices were gathered from different literature excluding 4 from this study. A number of literatures had been using multiple indices (around 5 to 11) to determine

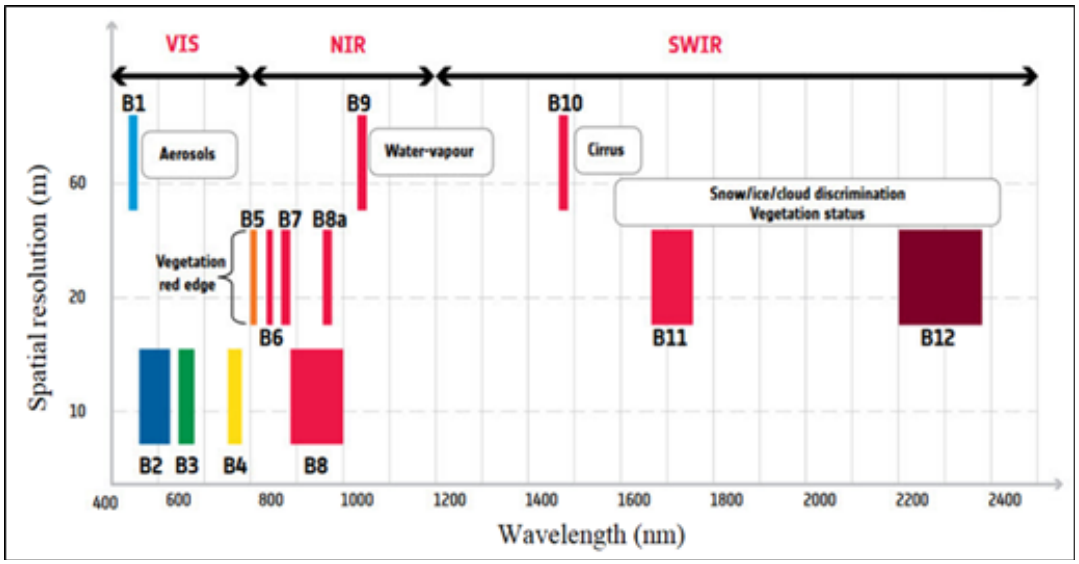

Figure 2. Sentinel-2's 13 spectral bands with corresponding bandwidth as illustrated per wavelength versus spatial resolution (Image source: https://esamultimedia.esa.int/docs/EarthObservation/Sentinel-2_ESA_Bulletin161.pdf)

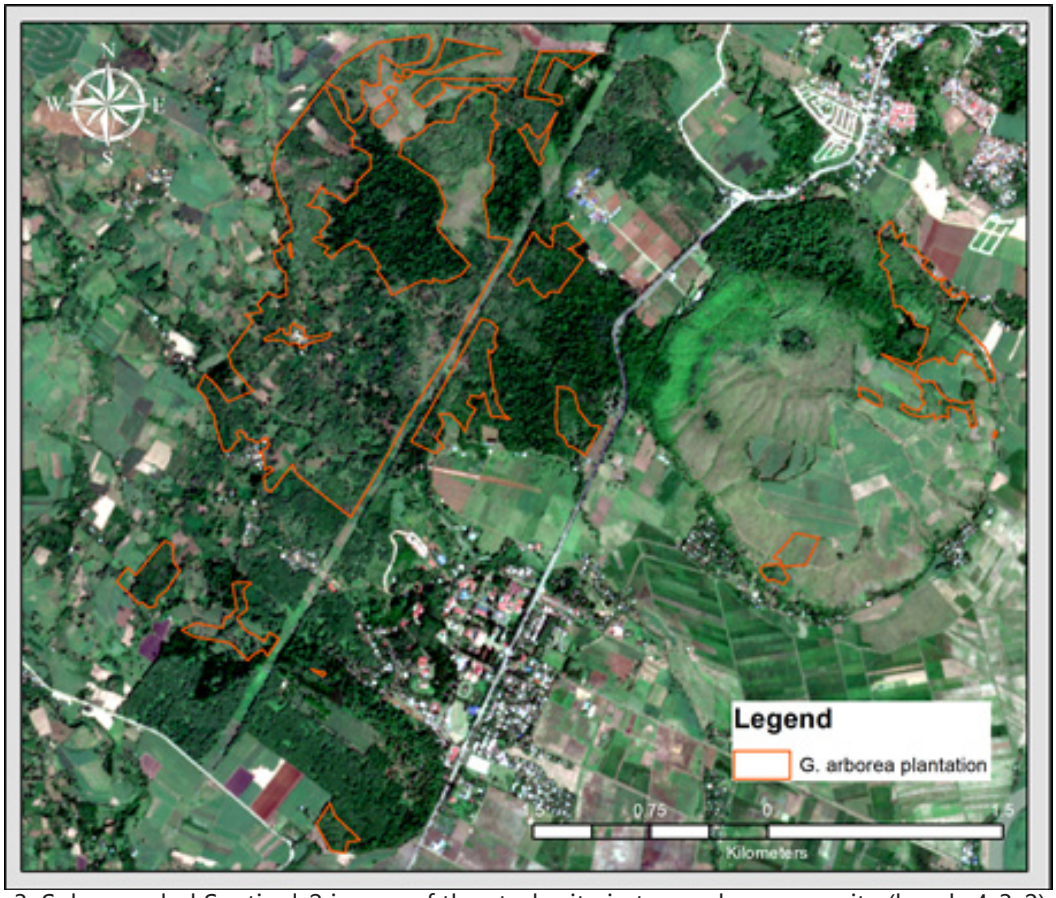

Figure 3. Sub-sampled Sentinel-2 image of the study site in true color composite (bands 4-3-2) dated December 23, 2019 to coincide with the time of the field survey

Table 1. Vegetation indices used in this study

Vegetation Index	Formula	Reference
Modified ratio vegetation index (MRVI)	(NIR/red-1)/√(NIR/red+1)	Chen and Cihlar, 1996
Enhanced vegetation index (EVI)	2.56((NIR-red)/(NIR+6(red)-7.5(blue)+1))	Liu and Huete, 1995
Normalized difference vegetation index (NDVI)	(NIR-red)/(NIR+red)	Rouse et al., 1973
Green NDVI (GNDVI)	(NIR-green)/(NIR+green)	Gitelson and Merzlyak, 1998
Soil adjusted vegetation index (SAVI)	((NIR-red)/(NIR-red+0.5))×1.5	Huete, 1988
Leaf chlorophyll index (LCI)	(NIR-VRE band 5)/(NIR+red)	Datt, 1999
Atmospherically resistant vegetation index (ARVI)	((NIR-red)-(NIR-blue))/((NIR+red)-(red-blue))	Thenkabail et al., 2002
Moisture adjusted vegetation index (MAVI)	(NIR-red)/(NIR+red+SWIR band 12)	Zhu et al, 2014
Inverted Red-edge Chlorophyll Index (IRCI)	(VRE band 7-red)/((VRE band 5)/(VRE band 6))	Frampton et al., 2013
$NDVI_{RE1}$	(VRE band 5-red)/(VRE band 5+red)	This study
$NDVI_{RE2}$	(VRE band 6-red)/(VRE band 6+red)	This study
$NDVI_{RE3}$	(VRE band 7-red)/(VRE band 7+red)	This study
$NDVI_{RE4}$	(VRE band 8a-red)/(VRE band 8a+red)	This study

Note: NIR = near infrared; VRE = vegetation red edge; SWIR = shortwave infrared

which is the best predictor of vegetation characteristics (e.g. Ali et al, 2020; Raper and Varco, 2015; Marcelli et al, 2020; Xie et al, 2015).

Data Processing and Statistical Analysis

Before any test was conducted, outliers were checked and omitted first. Plot-level correlation test, specifically Spearman's method, was performed between the various stand parameters and generated VIs to validate any relationships. Additionally, reflectance from bands 3 (green), 4 (red), 8 (NIR) and all the bands of vegetation red edge of S2 were also included in the correlation test. These bands and VIs are called S2 variables from here thereafter. In order to get the most practical values of S2 variables that best correspond to the field data, the same plot area was used for extracting their mean values. This was done by creating a circular buffer of 15 m for each geographic coordinate of all plots before overlaying them with the different S2 variables. Due to multicollinearity, the single variable with the highest correlation was further subjected to different curve estimation regression modeling with the total stem volume and BA. The model with the highest R^2 and the smallest standard error of estimate was chosen to estimate the spatial distribution of woody materials from trees.

RESULTS AND DISCUSSION

Stand Structure

The G. arborea plantation in the study has an average number of 309 ± 114.44 trees per hectare or a total number of 11,742 trees across the 38 plots sampled (Table 2). The trees were generally harvestable in size having mean DBH per plot of 0.30 ± 0.05 m and total height (TH) per plot of 15.71 ± 2.09 m. However, the average length of the usable wood portion of the trees (referred to as merchantable height, MH) was only about 60% of the TH which is equivalent to an average MH of 9.73 ± 2.64 m. The rest of the 40% was taken up by the crown cover, which had an average crown length (CL) of almost 6 m. Mean stem volume (SV) based on MH and TH respectively were estimated at 17.89 ± 9.64 m3 and 28.97 ± 2.29 m3, while the mean basal area (BA) per plot was 24.81 ± 10.19 m2/ha. The merchantable portions of trees in the area or potential yield can still be improved by 20% to 30% through regular pruning and thinning especially when the trees are still in the sapling stage. Tree plantations in the region and in the country more generally are poorly maintained resulting in a poor wood production rate of only about 632,574 m3 or 0.006 m3 per capita (FMB-DENR, 2019), which is more than 80 times lower than the world's average production rate of 0.5 m3 per capita (Bruinsma, 2002).

Vegetation Indices and Bands versus Field Data

After omitting the outliers, only 34 samples were left and subjected to statistical analysis. The result of the correlation test conducted between the S2 variables and stand parameters is summarized in Table 3. Only those with significant relationships were included in the table. Generally, all of the indices and bands involved are statistically correlated with the mean tree height, stem volume and BA of G. arborea. But the most sensitive index in terms of characterization is the LCI with coefficient of correlation ranging from moderate to slightly strong relationship ($R=0.44$ to 0.66, $p<.01$) mostly with those functions of the diameter like volume and basal area. Further, only 3 out of the 4 indices involving red edge bands proposed in this paper showed moderate correlation with only one stand parameter (mean height at 0.52 to 0.54, $p<.01$). Among the bands, the red edge bands of 7, 8 and 8a are responsive to heights and volume ($R=0.44$ to 0.55, $p<.01$). However, it was with band 5 (red edge) that registered the highest R at 0.61 with the mean diameter followed by band 3 (red). The mean tree height had the most number of correlations with the S2 variables (17 out of 20, or 85%) with NDVI registering the highest at 0.59.

Curve Estimation Models

Since the LCI recorded the highest correlation with the two important measure of wood density – the total volume and BA, these variables were subjected to both

Table 2. Descriptive statistics of stand parameters at plot level

Stand parameter	Mean	Standard deviation	Range	Minimum	Maximum
No. of trees/ha	309	114.44	538	141	679
DBH (m)	0.30	0.05	0.22	0.21	0.43
TH (m)	15.71	2.09	8.24	11.79	20.03
Maximum TH (m)	21.26	3.12	13.00	15.00	28.00
MH (m)	9.73	2.64	11.94	4.09	16.04
CL (m)	5.93	1.66	6.04	3.22	9.26
Total CL (m)	128.29	51.60	206.00	35.00	241.00
CC (%)	57.99	14.73	52.66	30.00	82.66
SVMH (m^3)	17.89	9.64	32.25	4.94	37.19
SVTH (m^3)	28.97	2.29	44.43	9.88	54.32
BA (m^2/ha)	24.81	10.19	36.55	8.82	45.37

linear and non-linear regression models. Table 4 shows that either power or exponential equations generated an adjusted R^2 of 0.43 with a standard error of less than 0.40. The paper by Günlü and Kadıoğulları (2018) in pine forest produced a lower R^2 of 0.36 with Landsat dataset using a stepwise linear regression. They were able to increased that to 0.54 by increasing the spatial resolution of the image dataset. Meanwhile, in spite of using the non-parametric random forest modeling with lidar technology to generate 3D models of trees, Brown et al (2022) still produced similar statistics for volume estimation (R^2=0.45).

Figure 4 below illustrates the curve lines based on the four equations fitted with the scatterplot of LCI-volume samples. It can be noticed that the volume only started to increased at 0.84 value of LCI, albeit quite noisy. Nevertheless, the trend of this graph is similar to the paper of Ali et al (2018) where NDVI and SAVI from Sentinel-2 were correlated with the aboveground biomass (AGB) of mixed stands. AGB of trees is typically computed from allometric equations involving the DBH.

Similarly, it was also either power or exponential equations that generated a better fit when predicting BA using the LCI (Table 5). Although its adjusted R^2 is a little lower than that of the volume, the standard error of estimate is lower at 0.34 only. Such outcome was validated by Günlü and Kadıoğulları (2018) using linear regression between the S2 variables against BA. The same authors generated an R^2 of 0.34 and 0.41 for Landsat and Quickbird, respectively. Similar results were seen from the study of Brown et al (2022) with R^2 of 0.36.

DISCUSSION

The relationships between tree structures and VIs or multispectral bands of this study is comparable with similar papers in the past. From Dos Reis et al (2018) in

Table 3. Spearman's correlation result between the VIs, bands and stand parameters

	mDBH	mTH	mMH	sCL	SVMH	SVTH	BA
MRVI	.282	.587**	.418*	.403*	.495**	.500**	.466**
EVI	.166	.546**	.461**	.371*	.484**	.487**	.413*
NDVI	.279	.594**	.425*	.398*	.500**	.499**	.466**
GNDVI	.353*	.547**	.415*	.367*	.540**	.528**	.503**
SAVI	.167	.486**	.435*	.319	.466**	.465**	.398*
LCI	.605**	.439**	.223	.368*	.630**	.650**	.659**
ARVI	.290	.587**	.389*	.410*	.468**	.479**	.450**
MAVI	.254	.530**	.428*	.326	.500**	.466**	.447**
IRCI	.343*	.571**	.424*	.415*	.540**	.543**	.516**
NDVIre1	-.308	.174	.235	.056	-.070	-.076	-.143
NDVIre2	.222	.515**	.373*	.348*	.384*	.393*	.365*
NDVIre3	.266	.545**	.400*	.354*	.421*	.419*	.398*
NDVIre4	.237	.537**	.372*	.375*	.390*	.395*	.373*
Band 3	-.549**	-.210	-.034	-.162	-.332	-.351*	-.422*
Band 4	-.317	-.387*	-.204	-.253	-.307	-.318	-.341*
Band 5	-.609**	-.272	-.055	-.161	-.360*	-.377*	-.436**
Band 6	-.010	.454**	.459**	.300	.421*	.404*	.342*
Band 7	.102	.548**	.532**	.349*	.520**	.485**	.438**
Band 8	.111	.517**	.483**	.291	.469**	.437**	.367*
Band 8a	.018	.524**	.546**	.324	.471**	.410*	.366*

*p < .05, **p<.01

Note: mDBH=mean DBH, mTH=mean total height, mMH=mean merchantable height; sCL=summation of crown length; SVMH=stem volume based on MH, SVTH=stem volume based on TH, BA=basal area

Table 4. Model summary and parameter estimates for total volume as the response variable

Equation	R^2	Adjusted R^2	Standard error of estimate	Sig	Parameter estimates		
					Constant	b1	b2
Linear	.398	.380	11.316	.000	-372.153	468.152	
Quadratic	.399	.361	11.489	.000	240.860	-969.338	842.290
Power	.445	.427	.397	.000	277.084	15.410	
Exponential	.444	.426	.398	.000	4.866E-06	18.058	

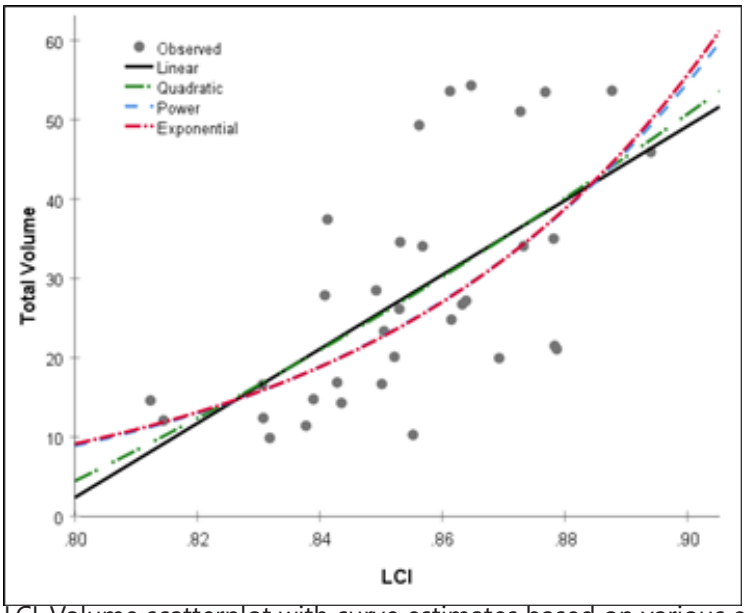

Figure 4. LCI-Volume scatterplot with curve estimates based on various equations

Table 5. Model summary and parameter estimates for BA as the response variable

Equation	R^2	Adjusted R^2	Standard error of estimate	Sig	Parameter estimates		
					Constant	b1	b2
Linear	.404	.386	8.291	.000	-272.531	347.314	
Quadratic	.407	.369	8.407	.000	508.698	-1484.635	1073.421
Power	.431	.413	.341	.000	167.430	12.865	
Exponential	.431	.413	.341	.000	5.576E-05	15.084	

Brazil, the NDVI of tree plantations from Landsat TM revealed an R values of 0.83 and 0.49 ($p<0.05$) for BA and tree volume as compared to 0.47 and 0.50 ($p<0.01$) in this study, respectively. Although their strongest correlation occurred between the normalizations of NIR and SWIR bands and BA at -0.91. In contrast, the highest R value in this paper is between LCI and BA with 0.66. Marcelli et al (2020), who also used Sentinel data in a poplar forest in Turkey, generated a correlation coefficient of 0.59 between NDVI and tree volume. Their highest correlation though was at 0.63 between tree volume and by simple ratioing of the NIR and SWIR bands.

Mutanga et al (2012) and Imran et al (2019) found a stronger relationship between AGB and NDVI if red edge bands were used compared to the broader NIR band (band 8) of S2 (R is up to 0.80). In contrast, the proposed NDVIs with red edge bands in this study had weak relationships with both volume and BA (0.36 to 0.42; $p<0.05$). Surprisingly, band 7 alone in this study had even higher correlations with the two parameters and is consistent with that of Imran et al (2019). On the other hand, Nguyen and Kappas (2020) reported that among the four spectral bands of SPOT-6 image, the red band has the strongest correlation with AGB conducted in a mixed forest including pines. Conversely, the red band in this paper is weakly correlated with only the mean height and BA. This could be attributable to the type of species being analyzed. The responses of indices and the bands involved are sometimes species-specific or restricted only to specific types of plants (Huete, 2004; Raper and Varco, 2015; Xie et al., 2015).

The LCI, developed by Datt in 1999, was originally used to determine the chlorophyll content of Eucalyptus species at leaf level. Accordingly, it was found to be a sensitive indicator of chlorophyll content in leaves and was less affected by scattering from the leaf surface and internal structure variation. Determination and analysis of chlorophyll content are crucial in studying vegetation health, forest growth or presence of stress as affected by diseases or insects (Yang et al, 2015; Gittelson et al, 2006; Sampson et al, 2003). Most of the remote sensing studies conducted in relation to chlorophyll assessment were done using airborne hyperspectral images which have narrower bands and higher resolution (e.g. Carmona et al, 2015; Zhang et al, 2008) in contrast to the one used in this paper. This is probably one of the reasons why the level of correlation between the field and RS datasets is only moderate. Moreover, stand conditions played important role in this kind of modeling as there were components captured by the satellite image but were not considered in the field data. For instance, the average canopy cover of the plots was less than 60% with a standard deviation of 15% and a minimum of 30%. Further, the average number of trees on per hectare basis from other studies (Ali et al, 2018; Günlü and Kadıoğulları, 2018) were at least doubled compared to this paper (309 versus 600 to 1000+ trees). All of these situations collectively affect the spectral characteristics as detected by the satellite sensors because soil and understories are visible through the canopy gaps. The NDVI, EVI and SAVI had been the earliest and widely

used indices for assessing vegetation growth and vigor. Hue and Su (2017) consider them as basic vegetation indices that exploit the characteristics of green vegetation having a generally low reflectance in the visible region particularly in the red portion (600-700 nm) but higher in the near-infrared (700-1100 nm). It is basically the same principle that is being followed by the other VIs in this study, although some were modified to lessen the effects of the atmosphere, soil background or both. The main issue with NDVI is that it tends to saturate as its value gets closer to 1. For instance, when the canopy cover is high and with dense vegetation, the biomass increases but the spectral index remains constant (Imran et al, 2019). This is most likely the reason why LCI in this paper is a better predictor of BA and volume than NDVI. LCI involved one of the red edge bands (Band 5) in the equation which is thought to be sensitive to the trees' structural and health condition. These findings had been corroborated by Mutanga et al (2012) where index with red edge bands had stronger correlation with the biomass compared to the conventional NDVI. The rest of the VIs were developed to investigate certain leaf pigments or to improve the estimation of specific vegetation parameters such as biomass, leaf area index (defined as the area of single leaf per area on the ground) and presence of moisture (Zheng and Moskal, 2009; Imran et al., 2020; Gao, 1996; Silleos et al., 2006).

Mapping Out Priority Areas for Harvesting

The LCI values within the G. arborea plantation were substituted to the non-linear power equation of the LCI-volume model to demonstrate the spatial distribution of the plantation's woody materials. The product was resampled to 27m to coincide with the area of the circular field plot and then reclassified into four categories based on the quantile value (figure 6). The categories pertain to the harvesting priorities where 1 and 4 in the map are the top and last priorities for cutting, respectively.

CONCLUSION

This study had just proven the usefulness of RS technology as an aid in identifying site parameters of the G. arborea plantation at landscape level significant to its growth and planning development. Since satellite images for the area are available on a regular basis (at least in the case of S2), the methodology introduced can be conducted yearly to monitor any changes in the plantation for adaptive management. As a result, plantation managers become more efficient in performing their task. Actual validation on the field, additional sampling plots and the use of non-parametric regression modeling or machine learning algorithm are recommended to further strengthen the analysis.

REFERENCES

Ali A., Ullah S., Bushra S., Ahmad N, Ali A. and Muhammad Awais Khan. (2018). Quantifying forest carbon stocks by integrating satellite images and forest inventory data. Austrian Journal of Forest Science, 2:93–117.

Barnes, E. M., Clarke, T. R., Richards, S. E., Colaizzi, P. D., Haberland, J., Kostrzewski, M., et al. (n.d.). Coincident detection of crop water stress, nitrogen status and canopy density using ground-based multispectral data. In: Proceedings of the Fifth International Conference on Precision Agriculture. Bloomington, MN, USA.

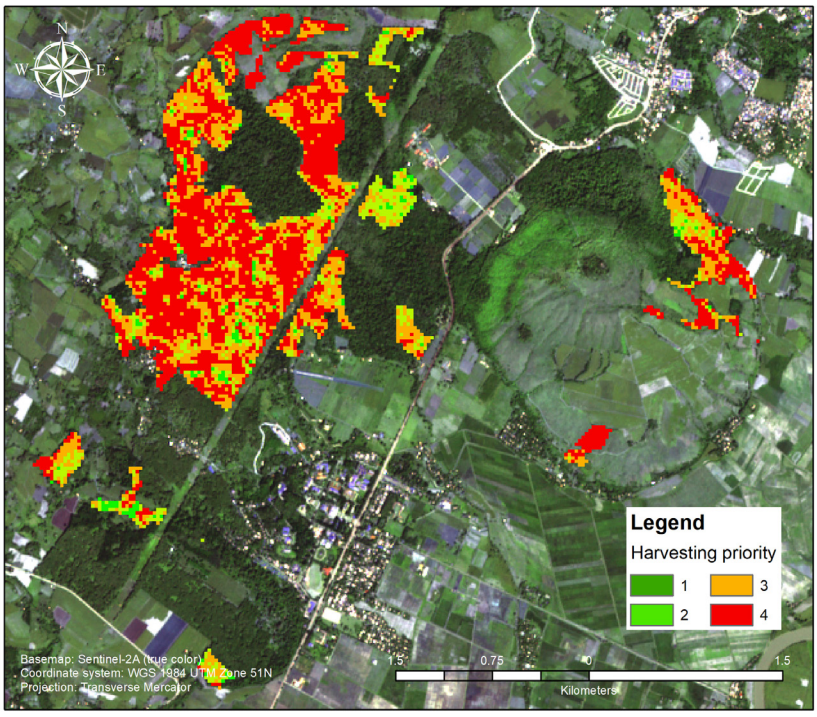

Figure 6. Resampled LCI-volume power equation model of G. arborea plantation for estimating which grids need to be harvested first where priorities 1 and 4 are the first and last to be cut (1 grid = 0.7 ha)

Beguet B., Chehata N., Boukir S. and D. Guyon. (2012). Retrieving Forest Structure Variables from Very High Resolution Satellite Images Using an Automatic Method. ISPRS Annals of the Photogrammetry, Remote Sensing and Spatial Information Sciences, Volume I-7. XXII ISPRS Congress, Melbourne, Australia.

Blackburn, G. A. (1998). Spectral indices for estimating photosynthetic pigment concentrations: A test using senescent tree leaves. International Journal of Remote Sensing, 19(4), 657-675.

Brown S., Narine L.L. and Gilbert J. (2022). Using Airborne Lidar, Multispectral Imagery and Field Inventory Data to Estimate Basal Area, Volume and Aboveground Biomass in Heterogeneous Mixed Species Forests: A Case Study in Southern Alabama. Remote Sensing, 14:2708. https://doi.org/10.3390/rs14112708

Bruinsma, J. (2002). World Agriculture: towards 2015/2030: Summary Report. Food and Agriculture Organization of the United Nations.

Chen, J. M., & J. Cihlar. (1996). Retrieving leaf area index of boreal conifer forests using Landsat TM images. Remote Sensing of Environment, 55, 153-162.

CMU CLUP. (2016). Central Mindanao University – Comprehensive Land Use Plan. University Town, Musuan, Bukidnon: CMU.

Curran, P. J., Dungan, J. L., & Gholz, H. L. (1990). Exploring the relationship between reflectance red edge and chlorophyll content in slash pine. Tree Physiology, 7(1-4), 33-48.

Datt, B. (1999). Remote Sensing of Water Content in Eucalyptus Leaves. Australian Journal of Botany, 47(6), 909-923.

DOST-PCAARD. (2018). Challenges and Recommendations in the Industrial Tree Plantations. Laguna, Philippines: A Policy Brief of the Department of Science and Technology Philippine Council for Agriculture, Aquatic and Natural Resources Research and Development.

Dos Reis A., Carvalho M., de Mello J., Gomide L., Filho AC and Fausto Acerbi Jr. (2018). Spatial prediction of basal area and volume in Eucalyptus stands using Landsat TM data: an assessment of prediction methods. New Zealand Journal of Forestry Science, 48:1. DOI 10.1186/s40490-017-0108-0

ESA. (2015). Sentinel-2 User Handbook. European Space Agency. Available online: https://sentinel.esa.int/documents/247904/685211/Sentinel-2_User_Handbook

FMB-DENR. (2019). Philippine Forestry Statistics. Forest Management Bureau – Department of Environment and Natural Resources. Available online: https://drive.google.com/file/d/1Cuy-Sup929NPoxqBdVcDml-3iYfG2Nhn/view

Frampton, W. J., Dash, J., Watmough, G., & Milton, E. J. (2013). Evaluating the capabilities of Sentinel-2 for quantitative estimation of biophysical variables in vegetation. ISPRS Journal of Photogrammetry and Remote Sensing, 82, 83-92.

Gao, B. C. (1996). NDWI - A normalized difference water index for remote sensing of vegetation liquid water from space. Remote Sensing of Environment, 58, 257-266.

Gebreslasie, M. T., Ahmed, F. B., & Aardt, J. N. (2020). Predicting forest structural attributes using ancillary data and ASTER satellite data. International Journal of Applied Earth Observation and Geoinformation, 12(1, Suppl.), 23-26.

Gitelson, A. A. (2004). Wide Dynamic Range Vegetation Index for Remote Quantification of Biophysical Characteristics of Vegetation. Journal of Plant Physiology, 161, 165-173.

Gitelson, A. A., & Merzlyak, M. N. (1998). Remote Sensing of Chlorophyll Concentration In Higher Plant Leaves. Advances in Space Research, 22(5), 689-692.

Gitelson, A., & Merzlyak, M. N. (1994). Spectral Reflectance Changes Associated with Autumn Senescence of Aesculus hippocastanum L. and Acer platanoides L. Leaves. Spectral Features and Relation to Chlorophyll Estimation. Journal of Plant Physiology, 143, 286-292.

Gittelson, A.A., Viña, A., Verma, S.B., Rundquist, D.C., Arkebauer, T.J., Keydan, G., Leavitt, B., Ciganda, V., Burba, G.G., Suyker, A.E. (2006). Relationship between gross primary production and chlorophyll content in crops: Implications for the synoptic monitoring of vegetation productivity. Journal of Geophysical Research: Atmospheres. 111:1984–2012.

Günlü A. and Ali İhsan Kadıoğulları. (2018). Modeling Forest Stand Attributes Using Landsat ETM+ and QuickBird Satellite Images in Western Turkey. Bosque 39(1): 49-59. DOI: 10.4067/S0717-92002018000100005

Huete, A. R. (1988). A soil adjusted vegetation index (SAVI). Remote Sensing of Environment, 25, 295-309.

Huete, A. R. (2004). Remote sensing for environmental monitoring. In Environmental monitoring and characterization (pp. 183-206). Academic Press.

Imran AB., Khan K, Ali N, Ahmad N, Ali A & K. Shah. (2019). Narrow band based and broadband derived vegetation indices using Sentinel-2 Imagery to Estimate Vegetation Biomass. Global Journal of Environmental Science and Management, 6(1): 97-108. DOI: 10.22034/gjesm.2020.01.08.

Jordan, C. F. (1969). Derivation of Leaf-Area Index from Quality of Light on the Forest Floor. Ecology, 50(4), 663-666.

Liu, H. Q., & Huete, A. R. (1995). A feedback based

modification of the NDV I to minimize canopy background and atmospheric noise. IEEE Transactions on Geoscience and Remote Sensing, 33, 457-465.

Marcelli A., Mattioli W., Puletti N., Chianucci F., Gianelle D., Grotti M., Chirici G., D'Amico G., Francini S., Travaglini D., Fattorini L. & Corona P. (2020). Large-scale two-phase estimation of wood production by poplar plantations exploiting Sentinel-2 data as auxiliary information. Silva Fennica, 54(2):10247, page 15. https://doi.org/10.14214/sf.10247

Mutanga, O., Adam, E. & Cho, M. (2012). High density biomass estimation for wetland vegetation using WorldView-2 imagery and random forest regression algorithm. International Journal of Applied Earth Observation and Geoinformation. 18:399-406. https://doi.org/10.1016/j.jag.2012.03.012.

Nguyen TD & Martin Kappas. (2020). Estimating the Aboveground Biomass of an Evergreen Broadleaf Forest in Xuan Lien Nature Reserve, Thanh Hoa, Vietnam, Using SPOT-6 Data and the Random Forest Algorithm. International Journal of Forestry Research, vol. 2020, Article ID 4216160, 13 pages. https://doi.org/10.1155/2020/4216160

Nguyen, H. T., Jones, S., Soto-Berelov, M., Haywood, A., & Hislop, S. (2020). Landsat Time-Series for Estimating Forest Aboveground Biomass and Its Dynamics across Space and Time: A Review. Remote Sensing, 12(1), 98.

Olpenda, A. (2019). Space Technology for Policy-Making and Management of Protected Mountain Range in Southern Philippines. International Journal of Geoinformatics, 15(3), 45–53. https://doi.org/10.52939/ijg.v15i3.1853

Olpenda, A. S. & Tulod, A. M. (2019). Establishment and diversity assessment of permanent monitoring plots in both natural and plantation forests in Southern Philippines. Journal of Biodiversity and Environmental Science., 15(1), 22-29.

Perez, G. J., Comiso, J. C., Aragones, L. V., Merida, H. C., & Ong, P. S. (2020). Reforestation and Deforestation in Northern Luzon, Philippines: Critical Issues as Observed from Space. Forests, 11(10), 1071.

Raper TB and JJ Varco. (2015). Canopy-scale wavelength and vegetative index sensitivities to cotton growth parameters and nitrogen status. Precision Agriculture, 16, 62–76. https://doi.org/10.1007/s11119-014-9383-4.

Richardson, A. D., Duigan, S. P., & Berlyn, G. P. (2002). An evaluation of noninvasive methods to estimate foliar chlorophyll content. New Phytologist, 153, 185-194.

Rojo, M. A., & Paquit, J. C. (2018). Incidence of Heart Rot in a University Owned Plantation Forest. Journal of Biodiversity and Environmental Science, 13(6), 146-151.

Rouse, J. W., Haas, R. H., Schell, J. A., & Deering, D. W. (1973). Monitoring vegetation systems in the Great Plains with ERTS. In 3rd ERTS Symposium (pp. 309-317). Greenbelt: NASA SP-351 I.

Sampson, P. H., Zarco-Tejada, P. J., Mohammed, G. H., Miller, J. R., & Noland, T. L. (2003). Hyperspectral remote sensing of forest condition: Estimating chlorophyll content in tolerant hardwoods. Forest Science, 49(3):381−391.

Silleos, G., Thomas, A., Ioannis, G. & Konstantinos, P. (2006). Vegetation indices: Advances made in biomass estimation and vegetation monitoring in the last 30 years. Geocarto International. 21:21-28.

Thenkabail, P. S., Smith, R. B., & De Pauw, E. (2002). Evaluation of narrowband and broadband vegetation indices for determining optimal hyperspectral wavebands for agricultural crop characterization. Photogrammetric Engineering And Remote Sensing, 68(6), 607-621.

Tulod, A. M., Casas, J. V., Marin, R. A., & Ejoc, J. B. (2017). Diversity of native woody regeneration in exotic tree plantations and natural forest in Southern Philippines. Forest Science and Technology, 13:1, 31-40.

Xie Q, Huang W, Dash J, Song X, Huang L, Zhao J, Wang Renhong. (2015). Evaluating the potential of vegetation indices for winter wheat LAI estimation under different fertilization and water conditions. Advances in Space Research. 56. 10.1016/j.asr.2015.09.022.

Zheng G & Moskal LM. (2009). Retrieving Leaf Area Index (LAI) Using Remote Sensing: Theories, Methods and Sensors. Sensors. 9(4):2719-2745. https://doi.org/10.3390/s90402719

Zhu, G., Ju, W., Chen, J. M., & Liu, Y. (2014). A Novel Moisture Adjusted Vegetation Index (MAVI) to Reduce Background Reflectance and Topographical Effects on LAI Retrieval. PLOS ONE, 9(7).

ACKNOWLEDGEMENT

The authors are grateful for the support of the CMU Administration, the Forest Resources Enterprise Office (FREO), research assistants and the students who conducted their theses in line with this paper.